Site-specific Inhibition of Glomerulonephritis Progression by Targeted Delivery of Dexamethasone to Glomerular Endothelium

Sigridur A. Ásgeirsdóttir, Jan A.A.M. Kamps, Hester I. Bakker, Peter J. Zwiers, Peter Heeringa, Karen van der Weide, Harry van Goor, Arjen H. Petersen, Henriëtte Morselt, Henk E. Moorlag, E. Steenbergen, Cees G. Kallenberg, Grietje Molema

University Medical Center Groningen (UMCG), University of Groningen, The Netherlands, Dept. of Pathology & Laboratory Medicine, Medical Biology Section (SAÁ, JAAMK, HIB, PJZ, PH, KvdW, AHP, HM, HEM, GM), Dept. of Pathology & Laboratory Medicine, Pathology Section (HvG), Radboud University Nijmegen Medical Centre, Nijmegen, The Netherlands, Dept. of Pathology (ES), and UMCG, Dept. of Clinical Immunology (CGK).

1

Running title: Immunoliposomal Delivery of Dexamethasone to Glomeruli

Corresponding author:

S.A. Ásgeirsdóttir

Department of Pathology & Laboratory Medicine, Medical Biology Section

Hanzeplein 1, 9713 GZ Groningen, The Netherlands

Phone: +31 50 3610229

Fax: +31 50 3619911

e-mail: s.a.asgeirsdottir@med.umcg.nl

The manuscript contains: 36 text pages, 2 Tables, 8 Figures, 41 References

Abstract: 179 words

Introduction: 330 words

Discussion: 790 words

Nonstandard Abbreviations:

Ab_{Esel}; anti E-selectin antibody, BUN; blood urea nitrogen, C_t; threshold cycle value,

dexa; dexamethasone, GBM; glomerular basement membrane, LDM; laser dissection

microscopy, PAS; periodic acid-Schiff base, PEG; polyethylene glycol

2

Abstract

Glomerulonephritis represents a group of renal diseases with glomerular inflammation as a common pathologic finding. Due to the underlying immunologic character of these disorders, they are frequently treated with glucocorticoids and cytotoxic immunosuppressive agents. Although effective, use of these compounds has limitations due to toxicity and systemic side effects. In the current study we tested the hypothesis that targeted delivery of dexamethasone (dexa) by immunoliposomes to activated glomerular endothelium decreases renal injury while preventing its systemic side effects. E-selectin was chosen as a target molecule based on its disease specific expression on activated glomerular endothelium in a mouse anti-glomerular basement membrane glomerulonephritis. Site selective delivery of Ab_{Esel}-liposomes encapsulated dexamethasone strongly reduced glomerular proinflammatory gene expression without affecting blood glucose levels, a severe side effect of administration of free dexamethasone. Dexa-Ab_{Esel}-liposomes reduced renal injury as shown by a reduction of blood ureum nitrogen levels, decreased glomerular crescent formation and downregulation of disease associated genes. Immunoliposomal drug delivery to glomerular endothelium presents a powerful new strategy for treatment of glomerulonephritis to sustain efficacy and prevent side effects of potent anti-inflammatory drugs.

Introduction

The glomerulonephritides comprise a spectrum of inflammatory diseases specifically
affecting the glomeruli (Eremina et al., 2003). In general, glomerular inflammation is
characterized by activation of various common pro-inflammatory pathways including
complement activation, production of pro-inflammatory cytokines, endothelial
activation and influx of circulating leukocytes (Falk et al., 2004). As a consequence,
glomerular injury and proteinuria develop.

Based on the underlying immunologic nature of glomerulonephritides, these disorders
are frequently treated with glucocorticosteroids in combination with cytotoxic agents
(Javaid and Quigg, 2005). Glucocorticosteroids and cytotoxic agents, such as
cyclophosphamide, are potent anti-inflammatory and immunosuppressive agents, but
have their limitation with regard to toxicity and side effects (Tam, 2006;Chadban and
Atkins, 2005). Identifying more effective and less toxic treatment for
glomerulonephritis still remains a major aim. One way to increase drug efficacy and
decrease side effects of treatment is to selectively deliver the therapeutic entity into
the diseased tissue. Endothelial cells have obtained considerable attention as targets
for this purpose (Ulbrich et al., 2003;Kuldo et al., 2005;Kamps et al., 1997). Not only
are endothelial cells in direct contact with the blood stream and consequently
accessible for systemically administered therapeutics, but, they also play an essential
role in the pathological process associated with glomerulonephritis. The interaction of
leukocytes with activated endothelial cells is well orchestrated via processes of
tethering and rolling, mediated by endothelial expression of P- and E-selectin,
followed by firm adhesion through interaction between integrins of the leukocytes,

4

and endothelial members of the immunoglobulin superfamily, including VCAM-1 and ICAM-1 (Vestweber, 2002).

Liposomes are high capacity drug carriers that, when modified with monoclonal antibodies, can be targeted to a selective target epitope of choice (Spragg et al., 1997;Kamps and Molema, 2006). Inflammation related cell adhesion molecules, including E-selectin and VCAM-1, are attractive candidates as target epitopes on activated endothelium because of their increased expression during inflammation and their predominant endothelial location.

The current study was designed to explore the feasibility of local immunoliposomal delivery of the glucocorticosteroid dexamethasone into activated glomerular endothelium in glomerulonephritis.

Material and Methods

Preparation of Iimmunoliposomes

Synthesis of immunoliposomes was as described earlier (Bartsch et al., 2005;Kamps

et al., 1996). In short, lipids from stock solutions of 1-Palmitoyl-2-oleoyl-sn-glycero-

3-phosphocholine (POPC), cholesterol, 1,2-distearoyl-sn-glycero-3-

phosphoethanolamine-N-[methoxy(polyethylene glycol)-2000] (DSPE-PEG) and 1,2-

distearoyl-sn-glycero-3-phosphoethanolamine-N-[methoxy(polyethylene glycol)-

2000]-maleimide (DSPE-PEG-Mal) in chloroform : methanol (9 : 1), were mixed in a

molar ratio of 55 : 40 : 4 : 1, dried under reduced nitrogen pressure, dissolved in

cyclohexane, and lyophilized. The lipids were then hydrated in HN buffer (10 mM

N-2-hydroxyethylpiperazine-N'-2-ethanesulfonic acid (Hepes), 135 mM NaCl, pH

6.7) or when appropriate in an aqueous solution of 75-100 mg/ml dexamethasone

disodium phosphate. The liposomes formed were sized by repeated extrusion (13

times) through polycarbonate filters (Costar, Cambridge MA, USA), pore size 50 nm,

using a high pressure extruder (Lipex, Vancouver, Canada). The monoclonal rat anti-

mouse E-selectin antibody, (MES-1, kindly provided by Dr. D. Brown, Celltech

group, UK) and irrelevant rat IgG (Sigma-Aldrich Chemie, Zwijndrecht, The

Netherlands) were thiolated by means of N-succinimidyl-S-acetylthioacetate, and

coupled to a maleimide group at the distal end of the polyethylene glycol chain (PEG)

by a sulfhydryl-maleimide coupling technique. The immunoliposomes were

characterized by determining protein content, using mouse IgG as a standard

(Peterson, 1977), and phospholipid phosphorus content (Bottcher et al., 1961). Total

liposomal lipid concentrations were adjusted for the amount of cholesterol present in

the liposome preparations. Per mol lipid 52.1 ± 25.6 g anti E-selectin antibody and

53.6 ± 23.1 g irrelevant rat IgG was coupled, respectively. Particle size was analyzed

by dynamic light scattering using a Nicomp model 370 submicron particle analyzer

(Santa Barbara, CA, USA) in the volume weighing model. The diameter size of

Ab_{Esel}-liposomes was 114.0 ± 31.1 nm and those of IgG-liposomes 103.3 ± 16.4 nm.

The number of antibody molecules coupled per liposome was calculated based on the

measured concentration (C_{Ab}) of antibody (g/mol lipid) and diameter of the

immunoliposomes (R) and the assumptions that the liposomes were approximately

spherical. From this, and literature values for specific lipid volume (V_{Ls}) of $1.25 nm^3$,

liposome bilayer thickness (d_{bl}) of 3.7 nm (Enoch and Strittmatter, 1979) and the

molecular weight of the antibody molecule (M_{Ab}) of 150 kDa, the number of

antibodies coupled to the liposomes was estimated by geometric arguments according

to the following formula: $\pi/6 * C_{Ab} * (3d_{bl} * R^2 - 3R * d_{bl}^2 + d_{bl}^3) * M_{Ab}^{-1} * V_{Ls}^{-1}$ (Adrian et

al., 2007) to be 20 Ab_{Esel} molecules per liposome and 17 IgG molecules per liposome.

The content of encapsulated dexamethasone disodium-phosphate (Bufa, Hilversum,

The Netherlands) was determined after Bligh and Dyer extraction in the resulting

methanol/H_2O phase by HPLC (Melgert et al., 2000). Per µmol lipid 55.4 ± 6.5 µg

dexamethasone was encapsulated.

Animals

C57bl/6 female mice were purchased from Harlan (Zeist, The Netherlands). Animals

were maintained on mouse chow and tap water *ad libitum* in a temperature-controlled

chamber at 24°C with a 12-hr light/dark cycle. All animal experiments were

performed upon approval of the local Animal Care and Use Committee of Groningen

University. After an adaptation period of one week, mice were allocated to the

experiments as described below.

Induction of Accelerated Anti-GBM Glomerulonephritis

The IgG fraction was isolated from polyclonal sheep anti-mouse GBM serum by HiTrap Sephadex-Protein G column (GE Healthcare Europe GmbH, Diegem, Belgium). Induction of anti-GBM glomerulonephritis was modified from the earlier described protocol (Assmann et al., 1985;Heeringa et al., 2000). In short, immunization was initiated by 100 µl (2 mg/ml) commercially available sheep IgG (Sigma-Aldrich Chemie, Zwijndrecht, The Netherlands) mixed with 100 µl complete Freund's adjuvant (BD Pharmingen, Alphen aan den Rijn, The Netherlands) and injected intraperitoneally. After 6.5 days glomerulonephritis was induced by *i.v.* injection with 1 mg sheep anti-mouse GBM antibodies and 200 ng recombinant mouse tumor necrosis factor alpha (TNFα; BioSource Europe, Nivelles, Belgium). The total volume injected was 200 µl. Mice were sacrificed at 2 h (n=12), 24 h (n=6), 48 h (n=9), 7 days (n=5) and 14 days (n=11). Organs were perfused with ice-cold phosphate buffered saline (PBS) and harvested. One kidney was fixed in 4% formaldehyde/PBS and embedded in paraffin for morphological analysis, the other kidney, and liver, spleen and heart were snap-frozen in liquid nitrogen and stored at -80°C.

Glomerulonephritis Development and Disease Progression

Five-µm cryosections were fixed in acetone for 10 minutes and incubated with fluorescein isothiocyanate (FITC)-labeled rabbit anti-sheep IgG or -anti-mouse IgG antibodies (DAKO, Glostrup, Denmark). Nuclear counterstaining was performed with 4',6-diamidino-2-phenylindole (DAPI; Boehringer, Mannheim, Germany). Sections were examined using a fluorescence microscope (DM RXA, Leica, Cambridge, UK) and Leica Q600 Qwin V01.06 software.

For morphological analysis of renal injury 4-μm formaldehyde fixed, paraffin

embedded sections were stained with periodic acid-Schiff base (PAS). The amount of

PAS-positive material within glomeruli was semiquantitatively scored as previously

described (Heeringa et al., 2000). A glomerular crescent score was determined for

each animal. Only glomeruli that had two or more layers of cells in Bowman's space

were considered crescent. The presence of PAS-positive material and glomerular

crescent were expressed as mean scores obtained by two experimentally blinded

observers counting between 50 and 100 glomeruli per kidney section.

Homing Studies and Pharmacological Effects of Targeted Delivery of Dexamethasone

Versus Free Dexamethasone

For homing studies and acute pharmacological effects, dexamethasone (Genfarma,

Maarsen, The Netherlands; 25 μg per mouse; n=7), Ab_{Esel}-liposomes (0.4 μmol lipid;

n=4), IgG-liposomes (0.4 μmol lipid; n=3) and Dexa-Ab_{Esel}-liposomes (0.4 μmol

lipid, 25 μg dexamethasone phosphate; n=6), respectively, were *i.v.* injected at the

onset of glomerulonephritis induction. To analyze pharmacological effects at day 14,

mice (n=6 per treatment) were *i.v.* injected twice with, respectively, Ab_{Esel}-liposomes,

Dexa-Ab_{Esel}-liposomes, Dexa-IgG-liposomes and free dexamethasone, at the onset of

glomerulonephritis induction, and at day 7 (dosages as above). In the group treated

with empty Ab_{Esel}-liposomes, one mouse lost more than 15% body weight and was

taken out of the experiment at day 4.

Blood and Urine Examinations

Blood urea nitrogen (BUN) was measured in plasma collected at the time of sacrifice

by an enzymatic degradation assay on a Vitros 250 automated analyzer (Johnson &

Johnson, South Brunswick, NJ). Glucose concentration was determined in plasma

using YSI 2300 STAT glucose oxidase analyzer. For the collection of urine mice were

placed for 24 h in individual metabolic cages. Urinary albumin content was measured

in 96-wells microplates (NalgeNUNC International Rochester, NY) with the mouse

albumin enzyme-linked immunosorbent assay (ELISA) quantitation kit (Bethyl

Laboratories, Montgomery, TX) using purified mouse albumin as a reference. Plasma

and urinary creatinine levels were measured by enzymatic colorimetric method using

Creatinine plus (Roche, Woerden, The Netherlands), which allows precise and

specific quantification of creatinine (Keppler et al., 2007). The creatinine clearance

(C_{Cr}) was calculated according to the formula $C_{Cr} = [Cr_{urine}] \times V_{olume\ urine}$ (ml per min)

$\times [Cr_{plasma}]^{-1}$.

Quantitative Gene Expression Analysis by Realtime RT-PCR

Total RNA was isolated from ten 8-µm cryosections with RNeasy mini kit (Qiagen

Benelux B.V., Venlo, The Netherlands) including a DNase treatment on the column.

RNA integrity was studied by gel electrophoresis and RNA yield (OD_{260}) and purity

(OD_{260}/ OD_{280}) were measured by ND-1000 UV-Vis Spectrophotometer (NanoDrop

Technologies, Rockland, DE, USA). One microgram RNA was reverse transcribed

using SuperscriptIII reverse transcriptase (Invitrogen, Breda, The Netherlands) and

random hexamer primers (Promega, Leiden, The Netherlands). Quantitative PCR

amplifications were performed according to manufacturers protocol on an ABI Prism

7900HT Sequence Detection System (Applied Biosystems, Applera Nederland,

Nieuwerkerk a/d IJssel, The Netherlands). Primers and probes for E-selectin, VCAM-

1 and ICAM-1 were purchased as customized assays from Applied Biosystems. These

primer/probes span multiple exons and were designed according to the same quality

criteria as the Assays-on-Demand primer/probes used. Sequences and accession

numbers are shown in Table 1. All PCR reactions were carried out in triplicate.

Relative quantitation of gene expression was calculated based on the comparative Ct

method ($\Delta Ct = Ct_{\text{gene of interest}} - Ct_{\text{housekeeping gene}}$). Comparison of gene expressions in

different samples was performed based on the differences in ΔCt of individual

samples ($\Delta\Delta Ct$).

Immunohistochemical Analysis of Cell Adhesion Molecules, Immune Cell Infiltrates

and Localization of Immunoliposomes

Five-μm cryosections were fixed in acetone for 10 min and incubated for 45 min with

primary rat anti-mouse monoclonal antibodies: anti-E-selectin (MES-1), anti-VCAM-

1 (clone M/K-2.7; ATCC, Manassas VA, USA) anti-neutrophil (NIMP-R14) and anti-

monocyte/macrophage (FA-11). Endogenous biotin was blocked by Biotin Blocking

System (Dako) and peroxidase activity was blocked by incubation with 0.1% H_2O_2 in

PBS for 10 min. Subsequently, sections were incubated for 1 h with biotin labeled

rabbit anti-rat antibodies (DAKO; dilution 1:300 in PBS) in the presence of 5%

normal mouse serum and 5% normal sheep serum, and incubated for 30 min with

Streptavidine-ABComplex-HRP (DAKO). Peroxidase activity was detected with 3-

amino-9-ethylcarbazole (AEC; Sigma-Aldrich Chemie) and sections were

counterstained with Mayer's hematoxylin (Klinipath, Duiven, The Netherlands).

Isotype matched controls were carried out for all primary antibodies and consistently

found to be devoid of staining. Immunostaining of E-selectin in glomeruli was

quantified by counting the number of glomerular cross sections expressing E-selectin.

Glomerular infiltrates were evaluated by counting the number of stained cells in

glomeruli. Results were expressed as mean scores obtained by two experimentally blinded observers counting between 50 and 100 glomeruli per mouse.

To analyze accumulation of immunoliposomes in kidney, heart, liver and spleen immunohistochemical staining for *i.v.* injected liposomal anti-E-selectin antibodies was performed as described above, except for omitting incubation with primary antibody. For quantitative analysis of staining of immunoliposomes in glomeruli morphometric analysis of 50 glomeruli per mouse was carried out using Leica QWin image analysis software. Numbers represent percentage of stained area within glomeruli.

Laser Dissection Microscopy (LDM) to Isolate Glomeruli

Five-μm cryosections were mounted on 1.35 μm thin polyethylene-naphtalene membranes attached to normal 1 mm slides (P.A.L.M. Microlaser Technology AG, Bernried, Germany), fixed in acetone (3 minutes) and stained with Mayer's hematoxylin (2 min, 25 μl per section), washed with DEPC-treated water (10 sec, 25 μl per section) and air-dried. Glomeruli were dissected using the Laser Robot Microbeam System (P.A.L.M. Microlaser Technology). Eight hundred dissected glomeruli were collected directly in RNA lysis buffer (Stratagene Europe, Amsterdam, The Netherlands) in the cap of a microcentrifuge tube via laser pressure catapulting. Extraction of total RNA and DNase treatment were carried out according to the protocol of StrataPrep total RNA microprep kit (Stratagene). Quantitative RT-PCR was carried out as described above.

Statistic Analysis

MOL #34140

Statistical significance of differences was studied by means of the two-sided Student's

t-test, assuming equal variances, except for semiquantitative scoring of PAS positive

material. In the latter, statistical significance of differences was calculated by Mann-

Witney nonparametric test. Differences were considered to be significant when $p <$

0.05

Results

Induction and Development of Glomerulonephritis

Injection of heterologous antibodies directed against GBM resulted in onset of

glomerulonephritis in mice preimmunized with non-specific sheep antibodies. We

adapted the classical accelerated anti-GBM glomerulonephritis model (Assmann et

al., 1985) by including TNFα in the anti-GBM antibody injection. This resulted in

fast, reproducible and progressive inflammation in the glomeruli, whereas TNFα or

anti-GBM antibodies alone did not result in significant leukocyte influx or glomerular

injury (data not shown). Figure 1 demonstrates the development of progressive

glomerulonephritis in our model at different time points from 2h to 2 weeks.

Glomerular depositions of sheep and mouse immunoglobulin were observed at all

time points (Fig. 1a) with formation of glomerular intracapillary PAS-positive

thrombus starting at 2 days (Fig. 1b,c). Additionally, mild extracapillary proliferation

and intratubular protein casts were noted, all indicative of glomerulonephritis

induction (Fig. 1b). Glomerular accumulations of PAS-positive material was highest

at 2 days and remained present for 14 days (Fig. 1c). Crescent formation was detected

at 7 and 14 days after disease induction (Fig. 1b,d). Two hrs after glomerulonephritis

induction, a peak of intraglomerular neutrophils was observed (Fig. 1e). The

glomerular accumulation of neutrophils subsequently decreased in time, which was

paralleled by an increase of intraglomerular monocytes (Fig. 1e), a time dependent

pattern that is characteristic for the experimental anti-GBM glomerulonephritis model

(Assmann et al., 1985;Masaki et al., 2003). Albuminuria was markedly increased after

induction of glomerulonephritis to > 50 mg per 24h at day 7 and 14, while untreated

mice secreted less than 0.1 mg albumin per 24 h (Fig. 1f). At the same time

glomerular filtration function deteriorated (Fig. 1g).

14

To further examine the disease process, expression of proinflammatory genes was analyzed by quantitative RT-PCR. First, treshold values (C_t) in kidneys of untreated mice were determined. Expression of cytokines and P- and E-selectin was low whereas VCAM-1, ICAM-1 and TGFβ were moderately expressed in healthy kidneys (Table 2). A rapid upregulation of cell adhesion molecules and cytokines was observed 2h after onset of glomerulonephritis (Fig. 2). The expression of cell adhesion molecules and cytokines was significantly higher compared to untreated animals throughout the experiment. Expression of the fibrosis related TGFβ enhanced slightly in time, indicative of ongoing glomerular injury and crescent formation (Border and Noble, 1994).

To characterize the proinflammatory gene expression profile specifically in glomeruli at the early stages of disease, we analyzed laser microdissected glomeruli. Interestingly, a spatial and temporal heterogenic regulation of proinflammatory genes in response to disease induction was observed. E-selectin was preferentially upregulated in glomeruli at all time points (Fig. 3a). Initially P-selectin was more abundantly expressed in the glomeruli than in total kidney isolates, whereas upregulation of VCAM-1 was more pronounced in the non-glomerular vascular compartments at all time points. Similarly to VCAM-1, glomerulonephritis induced expression of MCP1 was predominantly located outside the glomeruli (Fig. 3a). Gene expression data were corroborated by immunohistochemical analysis for E-selectin and VCAM-1 (Fig. 3b). E-selectin protein was solely produced in glomeruli whereas VCAM-1 was present in glomerular capillaries and in microvascular beds outside the glomeruli. The immunostaining of VCAM-1 was weak in glomeruli and stronger in arterioles. While E-selectin protein was undetectable in untreated mice, 2 h after disease induction 75 ± 5 % of all glomeruli were E-selectin positive. After 2

days the presence of glomerular E-selectin expression was decreased to 39 ± 13 % of all glomeruli.

I.V. Administered Ab$_{Esel}$- liposomes Selectively Homed to Hlomeruli

The disease specific glomerular expression of E-selectin provided it a promising target molecule on glomerular endothelial cells. Immunohistochemical staining demonstrated selective homing of *i.v.* administered immunoliposomes containing monoclonal anti-E-selectin antibodies (Ab$_{Esel}$) to the diseased glomeruli (Fig 4a). No staining was observed elsewhere in the kidney. This localization remained during disease development, although in time the staining became less pronounced. Glomerular staining of Ab$_{Esel}$-liposomes was detected at 2h in 93 ± 4%, at 1 day in 90 ± 1%, and at 2 days in 81 ± 6% of all glomeruli with approximately 10% of glomerular surface being positive for the specific immunoliposome (Fig. 4b). Control IgG-liposomes localized in glomeruli, likely due to local inflammation associated vascular permeability increase, but to a much lower extent (Fig 4a,b). No Ab$_{Esel}$-liposomes localized in the heart, whereas some association of Ab$_{Esel}$-liposomes was detected with cells in the red pulp in the spleen and with Kupffer cells in the liver, which reflects the regular elimination route of immunoliposomes in the body (data not shown).

To rule out the possibility that detecting the immunoliposomes using secondary antibody does not represent the liposomes themselves, we applied in a parallel experiment radioactive [^{3}H]cholesteryloleyl ether labeled Ab$_{Esel}$-liposomes or IgG-liposomes, and analyzed the kidney uptake of both liposome-preparations. The experiment demonstrated a targeting index of the lipid part of Ab$_{Esel}$-liposomes : IgG-liposomes of 3.6 : 1 (Ásgeirsdóttir et al., unpublished results), which corresponded

nicely to the glomerular surface staining by immunohistochemistry as shown in Fig

4b.

Based on this selective homing to inflamed glomerular endothelium Ab$_{Esel}$-liposomes

were next employed as carriers for a targeted delivery of dexamethasone to interfere

with glomerular endothelial cell activation and hence to counteract glomerulonephritis

development and progression.

Targeted Dexamethasone Exerted Strong, Local Pharmacological Eeffects Without

Alteration of Blood Glucose Level

Dexamethasone has pleiotropic anti-inflammatory effects, including an interaction

with the transcription factors NF-κB and AP-1, thereby preventing expression of

proinflammatory genes (Barnes, 2006). We therefore compared the effects of PEG-

ylated Ab$_{Esel}$-liposomes encapsulated dexamethasone and free dexamethasone using

mRNA levels of proinflammatory genes as read out. As expected, none of the

treatments prevented depositions of sheep and mouse immunoglobulin in glomeruli

(data not shown). Kidneys were harvested after 2h, a time point when

proinflammatory genes were robustly upregulated. Free dexamethasone significantly

inhibited gene expression induction of cell adhesion molecules and cytokines (Fig.

5a). Targeted liposomal delivery of dexamethasone similarly resulted in significant

downregulation of P- and E-selectin, whereas cytokine expression was slightly but not

statistically significantly, affected. No effects on proinflammatory gene expression

were observed in mice treated with empty Ab$_{Esel}$-liposomes (Fig. 5a).

Interestingly, expression of VCAM-1 was inhibited by free dexamethasone but not by

cell selective delivery into glomerular endothelium. Based on our data on

predominant non-glomerular expression of VCAM-1 (Fig. 3a) we hypothesized that

this discrepancy was due to local pharmacological effects of Dexa-Ab$_{Esel}$-liposomes in the glomeruli, combined with a relative low expression of VCAM-1 therein. We therefore studied the effect of Dexa-Ab$_{Esel}$-liposome on the expression levels of VCAM-1 in microdissected glomeruli and demonstrated that glomerular expression of VCAM-1 was indeed downregulated by Dexa-Ab$_{Esel}$-liposomes (Fig. 5b). Similarly, glomerular expression of MCP1 was downregulated by Dexa-Ab$_{Esel}$-liposomes, whereas no effect on MCP1 expression was observed in whole kidney isolates (Fig. 5). Downregulation of P- and E-selectin in microdissected glomeruli was comparable to that observed in whole kidney isolates (data not shown), corroborating the predominant expression of these cell adhesion molecules in glomeruli (Fig 3a). Dexamethasone is known to cause many side effects, such as osteoporosis, growth retardation in children, skin fragility and metabolic effects (Barnes, 2006). Hyperglycemia, caused by induction of hepatic gluconeogenesis and inhibition of cellular glucose uptake, is one of the most acute clinically relevant side effects of dexamethasone (Feldman-Billard et al., 2006;Hans et al., 2006;Weinstein et al., 1995). Indeed, in mice treated with free dexamethasone the plasma glucose concentration 2h after *i.v.* injection of the drug was significantly increased (Fig. 6). This was not observed in mice *i.v.* injected with dexamethasone encapsulated in immunoliposomes (Fig. 6).

Treatment with Dexa-Ab$_{Esel}$-liposomes Ameliorates Glomerulonephritis Progression
To study whether targeted inhibition of acute inflammatory gene expression in glomeruli would be able to counteract the occurrence of renal injury during glomerulonephritis development, mice were treated at day 0 and day 7 with free

dexamethasone, Dexa-Ab$_{Esel}$-liposomes, or empty Ab$_{Esel}$-liposomes and sacrificed at day 14.

Plasma BUN levels in mice treated with Dexa-Ab$_{Esel}$-liposomes were decreased as compared to levels in mice treated with Ab$_{Esel}$-liposomes (Fig. 7a). A similar reduction in BUN levels was observed in mice treated with free dexamethasone. A trend towards improved glomerular function exemplified by increased creatinine clearance was observed in both Dexa-Ab$_{Esel}$-liposomes and dexamethasone treated mice (Fig. 7b). Moreover, Dexa-Ab$_{Esel}$-liposomes were able to strongly inhibit the formation of crescents in glomeruli (Fig. 7c,d). The percentages of crescentic glomeruli decreased significantly from $30 \pm 4\%$ to $17 \pm 4\%$ (mean $\pm$ s.e.m.). Free dexamethasone showed a similar trend, however with a greater variation between mice (Fig. 7c). Overall, renal injury was notably counteracted by treatment with Dexa-Ab$_{Esel}$-liposomes, demonstrated by less glomerular lesions, intratubular protein casts, and tubulointerstitial damage (Fig. 7d). Control Dexa-IgG-liposomes that did end up in the kidney to a 4-fold lower extent than targeted Dexa-Ab$_{Esel}$-liposomes (see Fig. 4b), did reduce BUN levels to 13.4 ± 2.4 (mean $\pm$ s.e.m), a pharmacological effect which is most likely associated with inflammation related enhanced permeability and retention based passive accumulation and subsequent local slow drug release. In contrast, these non-targeted liposomes did not result in reduction of the formation of crescentic glomeruli ($29 \pm 3\%$; mean $\pm$ s.e.m), nor in improvement of creatinine clearance.

Concomitantly with improved renal function, treatment with Dexa-Ab$_{Esel}$-liposomes decreased the expression of disease related inflammatory genes at day 14. Expression levels of VCAM-1 and fibrosis related TGFβ were markedly lower in mice receiving Dexa-Ab$_{Esel}$-liposomes compared to empty Ab$_{Esel}$-liposomes (Fig. 8). Similarly, a

significant reduction in MCP1 and IL-6 mRNA levels was observed, whereas a trend

towards downregulation of IL-1β and TNFα was detected. Administration of free

dexamethasone resulted in significant downregulation of VCAM-1 and MCP1, while

TGFβ, IL-6, IL-1β and TNFα were not statistically significantly affected.

Discussion

In this study we demonstrate that targeted delivery of dexamethasone into glomerular endothelium by liposomes, modified with E-selectin specific monoclonal antibodies as homing device, selectively inhibited proinflammatory gene expression and improved renal function in progressive glomerulonephritis. Furthermore, the selective glomerular delivery of dexamethasone prevented unwanted systemic side effects which were observed after administration of free dexamethasone.

Anti-GBM crescentic glomerulonephritis can be treated with immunotherapy (Tam, 2006). Nonetheless, the need for more specific therapies is evident. The functional redundancy of molecules involved in leukocyte-endothelial cell interactions, as well as the complexity of inflammatory gene expression control and protein function, justifies cell specific therapeutic intervention with a broad pharmacological spectrum (Rosenkranz and Mayadas, 1999;Kuldo et al., 2005). Therefore we postulated that selective delivery of a potent anti-inflammatory drug with pleiotropic pharmacological effects into glomerular endothelium could exert a broad, yet local, inhibitory effect while preventing systemic side effects.

The current study is the first report describing a successful targeted delivery of drug loaded immunoliposomes to activated glomerular endothelial cells in glomerulonephritis in which local pharmacological activity did not interfere with vascular integrity. The local and disease specific expression of E-selectin on glomerular endothelium rendered it an excellent target molecule for drug delivery based therapy in glomerulonephritis. Previously, we reported a rapid receptor mediated internalization of anti E-selectin drug conjugates via E-selectin on activated endothelial cells (Kok et al., 2002;Asgeirsdottir et al., 2003;Everts et al., 2003). This intracellular delivery allows endothelial cell specific pharmacological interference of

regulatory mechanisms to control and inhibit the expression of proinflammatory

mediators such as cytokines and adhesion molecules, as demonstrated by our current

data.

The fact that elevated E-selectin expression has been detected in the kidney of

patients with IgA nephropathy, lupus nephritis and diabetic nephropathy supports the

clinical relevance of the development of E-selectin based drug targeting strategies

(Honkanen et al., 1998;Hirata et al., 1998). The use of endothelial target epitopes

other than E-selectin can, however, be taken into account. Immunoliposomes directed

toward VCAM-1 were internalized by activated endothelial cells *in vitro* (Voinea et

al., 2005), and *in vivo* demonstrated beneficial effects in an atherosclerosis mouse

model (Homem de Bittencourt PI Jr et al., 2006). The use of VCAM-1 selective

immunoliposomes in glomerulonephritis to interfere with microvascular endothelial

cells distinct from the glomerular capillaries is an attractive strategy, especially since

VCAM-1 is highly expressed throughout disease progression (Allen et al., 1999).

Laser capture microdissection is a valuable tool in (patho)physiology research as it, in

combination with qRT-PCR, allows the detection of local disease activity that

otherwise would be masked in analysis of a whole organ. For drug delivery research,

microdissection is also instrumental in revealing local molecular targets of the

therapeutic strategy studied. Using this approach we demonstrated that in our

glomerulonephritis model upregulation of proinflammatory genes differed between

the microvascular beds in the kidney. Strong upregulation of E-selectin was observed

on glomerular endothelium, whereas VCAM-1 and MCP1 expression was mainly

localized outside the glomeruli. Furthermore, RNA isolates of microdissected

glomeruli revealed local downregulation of VCAM-1 and MCP1 by Dexa-Ab$_{Esel}$-

liposomes, whereas the expression levels of these genes in whole kidney isolates were

not altered. Clearly, analysis in whole kidney isolates would lead to wrong conclusions about the pharmacological efficacy of Dexa-Ab$_{Esel}$-liposomes.

Targeted delivery to glomerular endothelium resulted in strong local pharmacological effects. In our study we used dexamethasone, a corticosteroid that is generally well tolerated after systemic administration, as a model drug to demonstrate proof of concept. However, today many potent anti inflammatory drugs do not make it through clinical trials because of severe side-effects (Peifer et al., 2006). For these classes of drugs the targeted delivery approach described in this study represents an important added value for future clinical applications. The challenge for the future drug delivery will be to formulate new chemical entities that are rapidly being discovered and are currently making their ways into basic research and clinical trials. These new drugs include tyrosine kinase inhibitors, MAPKinase inhibitors, and other agents interfering with proinflammatory signal transduction pathways (Bergers et al., 2003;Karin, 2006;Fabian et al., 2005). The recent observation that their molecular targets are fundamental in whole body homeostasis, makes their incorporation into cell-type specific drug delivery systems of essential value for clinical utility (Imming et al., 2006).

We showed that Dexa-Ab$_{Esel}$-liposomes were highly effective in improving renal function in glomerulonephritis, as reflected by reduced BUN levels, glomerular crescent formation and proinflammatory gene expression. Although free dexamethasone was also effective, encapsulation of dexamethasone into immunoliposomes prevented the occurrence of increased plasma glucose levels which was observed after administration of free dexamethasone. Hence, immunoliposomal delivery of potent drugs into inflamed microvascular endothelium maintains the pharmacological quality of the drug while eliminating systemic side effects and as

such represents a new therapeutic strategy for the treatment of glomerulonephritis.

MOL #34140

Reference List

Adrian JE, Kamps J A, Scherphof G L, Meijer D K, van Loenen-Weemaes A, Reker-Smit C, Terpstra P and Poelstra K (2007) A Novel Lipid-Based Drug Carrier Targeted to the Non-Parenchymal Cells, Including Hepatic Stellate Cells, in the Fibrotic Livers of Bile Duct Ligated Rats. *BBA Biomembranes* **(in press)**.

Allen AR, McHale J, Smith J, Cook H T, Karkar A, Haskard D O, Lobb R R and Pusey C D (1999) Endothelial Expression of VCAM-1 in Experimental Crescentic Nephritis and Effect of Antibodies to Very Late Antigen-4 or VCAM-1 on Glomerular Injury. *J Immunol* **162**:5519-5527.

Asgeirsdottir SA, Kok R J, Everts M, Meijer D K and Molema G (2003) Delivery of Pharmacologically Active Dexamethasone into Activated Endothelial Cells by Dexamethasone-Anti-E-Selectin Immunoconjugate. *Biochem Pharmacol* **65**:1729-1739.

Assmann KJ, Tangelder M M, Lange W P, Schrijver G and Koene R A (1985) Anti-GBM Nephritis in the Mouse: Severe Proteinuria in the Heterologous Phase. *Virchows Arch A Pathol Anat Histopathol* **406**:285-299.

Barnes PJ (2006) How Corticosteroids Control Inflammation: Quintiles Prize Lecture 2005. *Br J Pharmacol* **148**:245-254.

Bartsch M, Weeke-Klimp A H, Meijer D K, Scherphof G L and Kamps J A (2005) Cell-Specific Targeting of Lipid-Based Carriers for ODN and DNA. *J Liposome Res* **15**:59-92.

Bergers G, Song S, Meyer-Morse N, Bergsland E and Hanahan D (2003) Benefits of
Targeting Both Pericytes and Endothelial Cells in the Tumor Vasculature With
Kinase Inhibitors. *J Clin Invest* **111**:1287-1295.

Border WA and Noble N A (1994) Transforming Growth Factor Beta in Tissue
Fibrosis. *N Engl J Med* **331**:1286-1292.

Bottcher CDF, Van Gent C M and Pries C (1961) Rapid and Sensitive Submicro
Phosphorus Determination. *Anal Chim Acta* **24**:203-204.

Chadban SJ and Atkins R C (2005) Glomerulonephritis. *Lancet* **365**:1797-1806.

Enoch HG and Strittmatter P (1979) Formation and Properties of 1000-A-Diameter,
Single-Bilayer Phospholipid Vesicles. *Proc Natl Acad Sci USA* **76**:145-149.

Eremina V, Sood M, Haigh J, Nagy A, Lajoie G, Ferrara N, Gerber H P, Kikkawa Y,
Miner J H and Quaggin S E (2003) Glomerular-Specific Alterations of VEGF-A
Expression Lead to Distinct Congenital and Acquired Renal Diseases. *J Clin Invest*
111:707-716.

Everts M, Koning G A, Kok R J, Asgeirsdottir S A, Vestweber D, Meijer D K, Storm
G and Molema G (2003) In Vitro Cellular Handling and in Vivo Targeting of E-
Selectin-Directed Immunoconjugates and Immunoliposomes Used for Drug Delivery
to Inflamed Endothelium. *Pharm Res* **20**:64-72.

Fabian MA, Biggs W H, III, Treiber D K, Atteridge C E, Azimioara M D, Benedetti
M G, Carter T A, Ciceri P, Edeen P T, Floyd M, Ford J M, Galvin M, Gerlach J L,
Grotzfeld R M, Herrgard S, Insko D E, Insko M A, Lai A G, Lelias J M, Mehta S A,
Milanov Z V, Velasco A M, Wodicka L M, Patel H K, Zarrinkar P P and Lockhart D

J (2005) A Small Molecule-Kinase Interaction Map for Clinical Kinase Inhibitors. *Nat Biotechnol* **23**:329-336.

Falk RJ, Jenette J.C. and Nachmann P.H. (2004) Primary Glomerular Disease, in *The Kidney* (Brenner B.M ed) pp 1293-1380, Saunders, Philadelphia W.B.

Feldman-Billard S, Du Pasquier-Fediaevsky L and Heron E (2006) Hyperglycemia After Repeated Periocular Dexamethasone Injections in Patients With Diabetes. *Ophthalmology* **113**:1720-1723.

Hans P, Vanthuyne A, Dewandre P Y, Brichant J F and Bonhomme V (2006) Blood Glucose Concentration Profile After 10 Mg Dexamethasone in Non-Diabetic and Type 2 Diabetic Patients Undergoing Abdominal Surgery. *Br J Anaesth* **97**:164-170.

Heeringa P, Van Goor H, Itoh-Lindstrom Y, Maeda N, Falk R J, Assmann K J, Kallenberg C G and Jennette J C (2000) Lack of Endothelial Nitric Oxide Synthase Aggravates Murine Accelerated Anti-Glomerular Basement Membrane Glomerulonephritis. *Am J Pathol* **156**:879-888.

Hirata K, Shikata K, Matsuda M, Akiyama K, Sugimoto H, Kushiro M and Makino H (1998) Increased Expression of Selectins in Kidneys of Patients With Diabetic Nephropathy. *Diabetologia* **41**:185-192.

Homem de Bittencourt PI Jr, Lagranha D J, Maslinkiewicz A, Senna S M, Tavares A M, Baldissera L P, Janner D R, Peralta J S, Bock P M, Gutierrez L L, Scola G, Heck T G, Krause M S, Cruz L A, Abdalla D S, Lagranha C J, Lima T and Curi R (2006) LipoCardium: Endothelium-Directed Cyclopentenone Prostaglandin-Based Liposome Formulation That Completely Reverses Atherosclerotic Lesions. *Atherosclerosis* **..**

Honkanen E, von Willebrand E, Teppo A M, Tornroth T and Gronhagen-Riska C (1998) Adhesion Molecules and Urinary Tumor Necrosis Factor-Alpha in Idiopathic Membranous Glomerulonephritis. *Kidney Int* **53**:909-917.

Imming P, Sinning C and Meyer A (2006) Drugs, Their Targets and the Nature and Number of Drug Targets. *Nat Rev Drug Discov* **5**:821-834.

Javaid B and Quigg R J (2005) Treatment of Glomerulonephritis: Will We Ever Have Options Other Than Steroids and Cytotoxics? *Kidney Int* **67**:1692-1703.

Kamps JA and Molema G (2006) Targeting Liposomes to Endothelial Cells in Inflammatory Diseases, in *Liposome Technology, Volume III: Interactions of Liposomes With the Biological Milieu* (Gregoriadis G ed) pp 127-150, CRC Press.

Kamps JAAM, Morselt H W M, Swart P J, Meijer D K F and Scherphof G L (1997) Massive Targeting of Liposomes, Surface-Modified With Anionized Albumins, to Hepatic Endothelial Cells. *Proc Natl Acad Sci USA* **94**:11681-11685.

Kamps JAAM, Swart P J, Morselt H W M, Pauwels R, de Béthune M-P, De Clercq E, Meijer D K F and Scherphof G L (1996) Preparation and Characterization of Conjugates of (Modified) Human Serum Albumin and Liposomes: Drug Carriers With an Intrinsic Anti-HIV Activity. *Bba-Biomembranes* **1278**:183-190.

Karin M (2006) Nuclear Factor-KappaB in Cancer Development and Progression. *Nature* **441**:431-436.

Keppler A, Gretz N, Schmidt R, Kloetzer H M, Groene H J, Lelongt B, Meyer M, Sadick M and Pill J (2007) Plasma Creatinine Determination in Mice and Rats: An

Enzymatic Method Compares Favorably With a High-Performance Liquid Chromatography Assay. *Kidney Int* **71**:74-78.

Kok RJ, Everts M, Asgeirsdottir S A, Meijer D K and Molema G (2002) Cellular Handling of a Dexamethasone-Anti-E-Selectin Immunoconjugate by Activated Endothelial Cells: Comparison With Free Dexamethasone. *Pharm Res* **19**:1731-1736.

Kuldo JM, Ogawara K I, Werner N, Asgeirsdottir S A, Kamps J A, Kok R J and Molema G (2005) Molecular Pathways of Endothelial Cell Activation for (Targeted) Pharmacological Intervention of Chronic Inflammatory Diseases. *Curr Vasc Pharmacol* **3**:11-39.

Masaki T, Chow F, Nikolic-Paterson D J, Atkins R C and Tesch G H (2003) Heterogeneity of Antigen Expression Explains Controversy Over Glomerular Macrophage Accumulation in Mouse Glomerulonephritis. *Nephrol Dial Transplant* **18**:178-181.

Melgert BN, Olinga P, Jack V K, Molema G, Meijer D K F and Poelstra K (2000) Dexamethasone Coupled to Albumin Is Selectively Taken Up by Rat Nonparenchymal Liver Cells and Attenuates LPS-Induced Activation of Hepatic Cells. *J Hepatol* **32**:603-611.

Peifer C, Wagner G and Laufer S (2006) New Approaches to the Treatment of Inflammatory Disorders Small Molecule Inhibitors of P38 MAP Kinase. *Curr Top Med Chem* **6**:113-149.

Peterson GL (1977) A Simplification of the Protein Assay Method of Lowry Et Al. Which Is More Generally Applicable. *Anal Biochem* **83**:346-356.

Rosenkranz AR and Mayadas T N (1999) Leukocyte-Endothelial Cell Interactions - Lessons From Knockout Mice. *Exp Nephrol* **7**:125-136.

Spragg DD, Alford D R, Greferath R, Larsen C E, Lee K D, Gurtner G C, Cybulsky M I, Tosi P F, Nicolau C and Gimbrone M A (1997) Immunotargeting of Liposomes to Activated Vascular Endothelial Cells: A Strategy for Site-Selective Delivery in the Cardiovascular System. *Proc Natl Acad Sci USA* **94**:8795-8800.

Tam FW (2006) Current Pharmacotherapy for the Treatment of Crescentic Glomerulonephritis. *Expert Opin Investig Drugs* **15**:1353-1369.

Ulbrich H, Eriksson E E and Lindbom L (2003) Leukocyte and Endothelial Cell Adhesion Molecules As Targets for Therapeutic Interventions in Inflammatory Disease. *Trends Pharmacol Sci* **24**:640-647.

Vestweber D (2002) Regulation of Endothelial Cell Contacts During Leukocyte Extravasation. *Curr Op Cell Biol* **14**:587-593.

Voinea M, Manduteanu I, Dragomir E, Capraru M and Simionescu M (2005) Immunoliposomes Directed Toward VCAM-1 Interact Specifically With Activated Endothelial Cells--a Potential Tool for Specific Drug Delivery. *Pharm Res* **22**:1906-1917.

Weinstein SP, Paquin T, Pritsker A and Haber R S (1995) Glucocorticoid-Induced Insulin Resistance: Dexamethasone Inhibits the Activation of Glucose Transport in Rat Skeletal Muscle by Both Insulin- and Non-Insulin-Related Stimuli. *Diabetes* **44**:441-445.

Footnotes

The work was supported by grants from the Dutch Kidney Foundation (C01.1988 and

C04.2080).

Legends

Figure 1

Development of glomerulonephritis. (a) Glomerular deposition of sheep (left) and mouse (right) immunoglobulin at 1 day after glomerulonephritis induction (top panels). Immunofluorescent staining along the glomerular capillary wall was observed at all time points from 2h until 14 days. No staining was observed in healthy control mice (bottom panels). Nuclear counterstaining was performed with DAPI. (b) Light microscopy (PAS stain) of kidney from untreated mouse (top), and mice sacrificed 2 (middle) and 14 days (below) after induction of glomerulonephritis. Arrows indicate glomerular thrombus formation at day 2 and crescent formation at day 14. Inserts indicate a normal glomerulus with open capillaries and Bowman capsule (top), PAS-positive glomerulus with intracapillary thrombus (middle) and glomerular crescent formation (below). (c) Semiquantitative scoring of glomerular deposits of PAS-positive material as a measure of glomerular injury. (d) Presence of glomerular crescents was observed at 7 and 14 days after glomerulonephritis induction. (e) Glomerular infiltration of neutrophils and monocytes. (f) Development of albuminuria after induction of glomerulonephritis. (g) Blood urea nitrogen (BUN) levels after induction of glomerulonephritis. BUN levels were not determined (n.d.) at day 7. Data in (c) – (g) are presented as mean values $\pm$ s.e.m. of 5 – 12 animals per treatment. *, $p < 0.05$ compared to healthy control mice in (c), (d), (f), and (g).

Figure 2

Quantitative gene expression analysis of the cell adhesion molecules P- and E-selectin, VCAM-1, and ICAM-1, cytokines TNFα, IL-1β, IL-6, MCP1, and TGFβ in kidney of untreated mice (-), and at 2 h, and 1, 2, 7, and 14 days after induction of

glomerulonephritis. Expression levels of mRNA in untreated mice were arbitrarily set

at one. Data are presented as mean values ± s.e.m. of 5 - 12 animals per treatment.

*, $p < 0.05$ compared to non-treated animals.

Figure 3

Glomerular upregulation of cell adhesion molecules after induction of

glomerulonephritis. (a) Upregulation of P- and E-selectin, VCAM-1 and MCP1 in

microdissected glomeruli and total kidney isolates at 2h, 1 and 2 days after

glomerulonephritis induction. Expression levels of mRNA in untreated mice (-) were

arbitrarily set at one for total kidney isolates and microdissected glomeruli,

respectively. Data are presented as mean values ± s.e.m. of 6 animals per treatment.

*, $p < 0.05$ upregulation in glomeruli compared to whole kidney isolates. (b)

Immunohistochemical staining with anti-E-selectin antibodies, anti-VCAM-1

antibodies, and isotype matched control antibodies at 2h after glomerulonephritis

induction. Asterisk indicates arteriole, arrowhead glomerulus, arrow venule.

Figure 4

Intravenously injected Ab_{Esel}-liposomes selectively homed to glomeruli at the onset of

glomerulonephritis. (a) Immunohistochemical detection of Ab_{Esel}-liposomes (top

panel) and control IgG-liposomes (lower panel) 2h after glomerulonephritis induction.

(b) Quantitative morphometric analysis of intraglomerular immunohistochemical

staining of control IgG-liposomes and Ab_{Esel}-liposomes. Values indicate mean ±

s.e.m. of 3 animals per treatment group. *, $p < 0.05$ compared to control Ig-liposomes.

#, no significant difference was observed between Ab_{Esel}-liposomes at different time

points.

Figure 5

Dexamethasone and Dexa-Ab$_{Esel}$-liposomes strongly downregulated proinflammatory gene expression in glomerulonephritis. (a) Gene expression levels in whole kidney isolates of untreated mice and 2 h after induction of glomerulonephritis in the absence or presence of dexamethasone, Dexa-Ab$_{Esel}$-liposomes and empty Ab$_{Esel}$-liposomes, respectively. Expression levels of mRNA in untreated mice were arbitrarily set at one. Data are presented as mean values ± s.e.m. of 4 - 12 mice, *, $p < 0.05$. (b) Downregulation of glomerular expression of VCAM-1 and MCP1 by Dexa-Ab$_{Esel}$-liposomes. RNA was isolated from microdissected glomeruli. Expression levels of mRNA in untreated mice (hatched bar) were arbitrarily set at one. Disease associated glomerular expression (black bar) of VCAM-1 and MCP1 was prevented by treatment with Dexa-Ab$_{Esel}$-liposomes (white bar). Data are presented as mean values ± s.e.m. of 6 mice, *, $p < 0.05$

Figure 6

Increased plasma glucose levels in mice treated with free dexamethasone, while Dexa-Ab$_{Esel}$-liposomes were devoid of this systemic side effect. Control mice (-): 2h glomerulonephritis induction without drug treatment. Values represent mean ± s.e.m. of 6 -12 mice, *, $p < 0.05$.

Figure 7

Selective delivery of dexamethasone into glomerular endothelial cells reduced renal injury during progression of glomerulonephritis. Mice were *i.v.* injected at day 0 and 7 with empty Ab$_{Esel}$-liposomes (○), Dexa-Ab$_{Esel}$-liposomes (●) and free

dexamethasone ($\blacktriangledown$). (a) Plasma BUN levels at day 14 after glomerulonephritis induction were reduced in mice treated with Dexa-Ab$_{Esel}$-liposomes and dexamethasone. (b) A trend towards increased creatinine clearance at day 14 after glomerulonephritis induction was observed in mice treated with Dexa-Ab$_{Esel}$-liposomes and dexamethasone. (c) Glomerular crescent formation at day 14 after glomerulonephritis induction was significantly reduced in mice treated with Dexa-Ab$_{Esel}$-liposomes. (d) Representative PAS staining of kidney induction from mice treated with empty Ab$_{Esel}$-liposomes (left panel) and Dexa-Ab$_{Esel}$-liposomes (right panel) at day 14 after glomerulonephritis. The frequency of glomerular crescent formation (arrows), intratubular protein casts and tubulointerstitial injury were reduced in the Dexa-Ab$_{Esel}$-liposome treated mice.

Figure 8

Targeting dexamethasone to glomerular endothelium reduced expression of proinflammatory genes during progression of glomerulonephritis. Mice were *i.v.* injected at days 0 and 7 of glomerulonephritis development with empty Ab$_{Esel}$-liposomes (○), Dexa- Ab$_{Esel}$-liposomes (●) and free dexamethasone ($\blacktriangledown$). Gene expression was analyzed in whole kidney isolates at day 14. Expression levels of mRNA in healthy control mice (■) were arbitrarily set at one.

36

MOL #34140

Table 1: Primers used for quantitative RT-PCR

E-selectin	
forward	CAACGTCTAGGTTCAAAACAATCAG
probe	CACAAATGCATCGTGGGA
reverse	TTAAGCAGGCAAGAGGAACCA
VCAM-1	
forward	TGAAGTTGGCTCACAATTAAGAAGTT
probe	AACACTTGATGTAAAAGGA
reverse	TGCGCAGTAGAGTGCAAGGA
ICAM-1	
forward	ATGGGAATGTCACCAGGAATG
probe	CAGTACTGTACCACTCTC
reverse	GCACCAGAATGATTATAGTCCAGTTATT
P-selectin	Mm00441295_m1 (Applied Biosystems)
TNFα	Mm00443258_m1 (Applied Biosystems)
IL-1β	Mm00434228_m1 (Applied Biosystems)
IL-6	Mm00446190_m1 (Applied Biosystems)
MCP1	Mm00441242_m1 (Applied Biosystems)
TGFβ	Mm00441724_m1 (Applied Biosystems)
GAPDH	Mm99999915_g1 (Applied Biosystems)

37

Table 2: mRNA levels of proinflammatory genes in kidney of healthy control mice based on the number of cycles necessary for a fixed threshold value* (C_t) in quantitative RT-PCR. Values represent mean $C_t \pm$ SD, n = 3.

GAPDH (house keeping gene)	19.4 ± 0.5
P-selectin	33.0 ± 0.6
E-selectin	31.3 ± 0.6
VCAM-1	27.5 ± 0.5
ICAM-1	27.3 ± 0.5
TNFα	31.9 ± 0.5
IL-1β	32.5 ± 0.7
MCP1	32.0 ± 0.4
TGFβ	26.3 ± 0.6

* Higher C_t value represents lower expression level. One C_t value difference = 2 fold expression level difference.
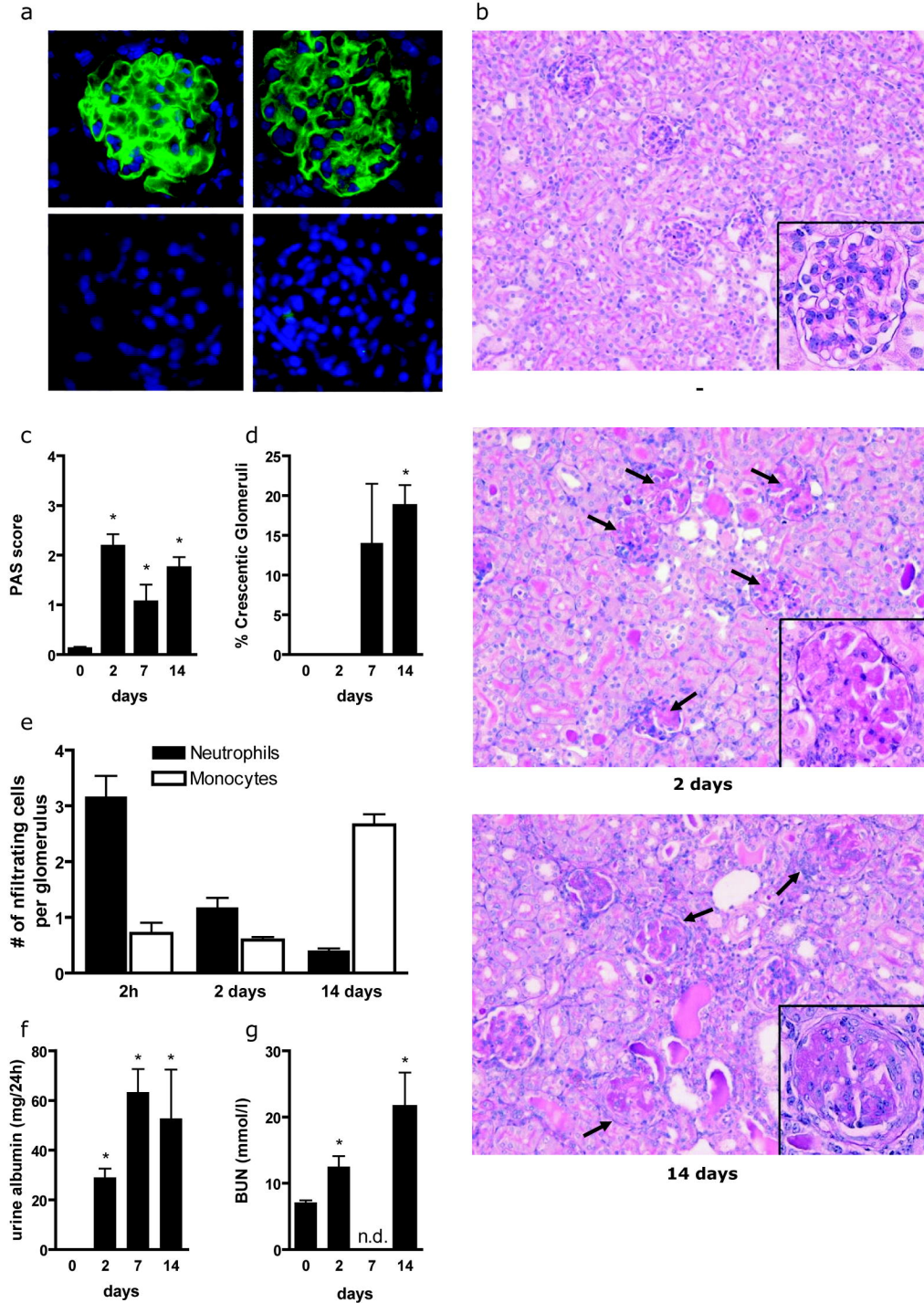
Figure 1

Figure 2

Figure 3

a

b

glomerular surface stained (%)

IgG-Lip | Ab$_{Esel}$-Lip

* #

2h | 2h | 1 | 2 days

after glomerulonephritis induction
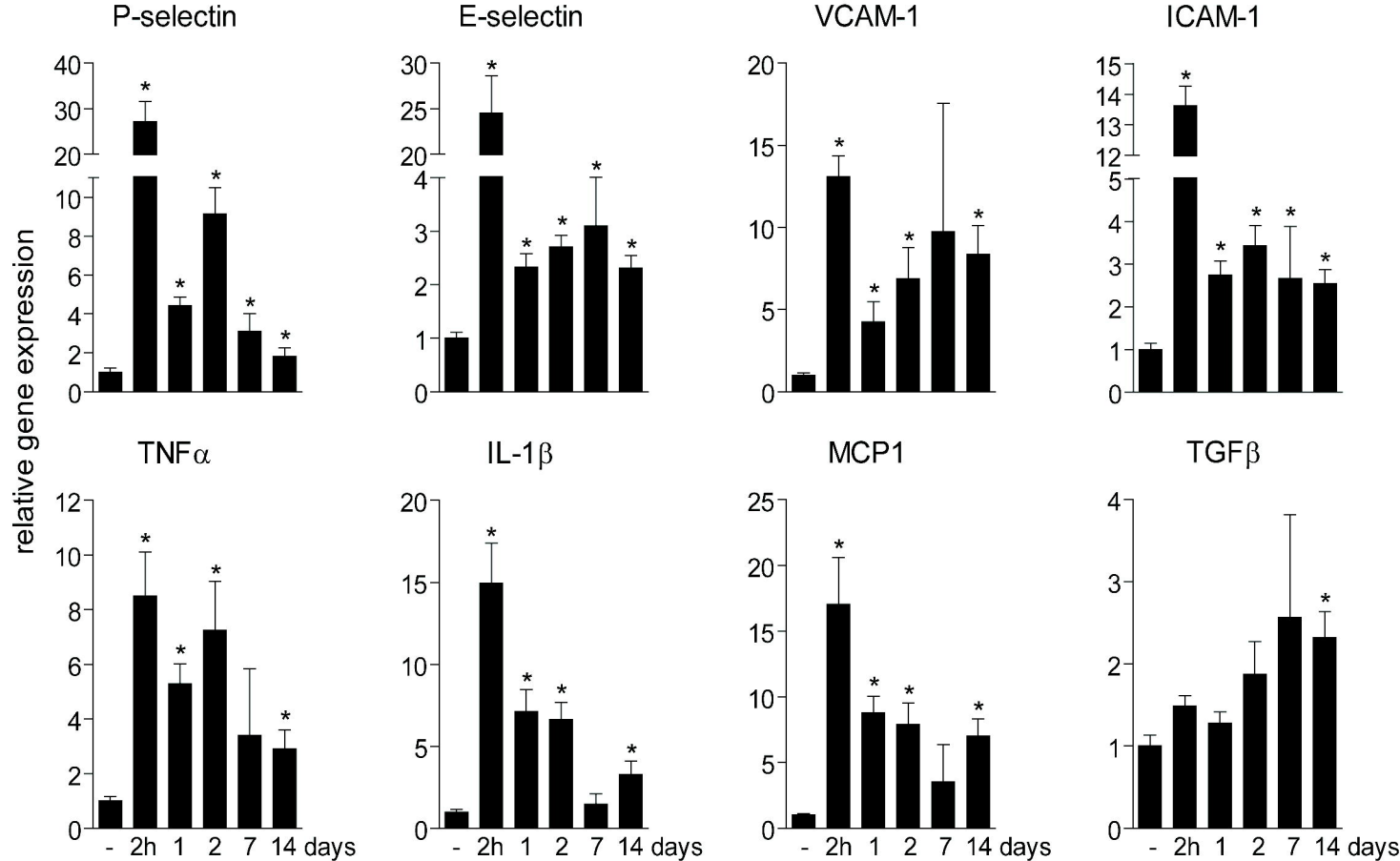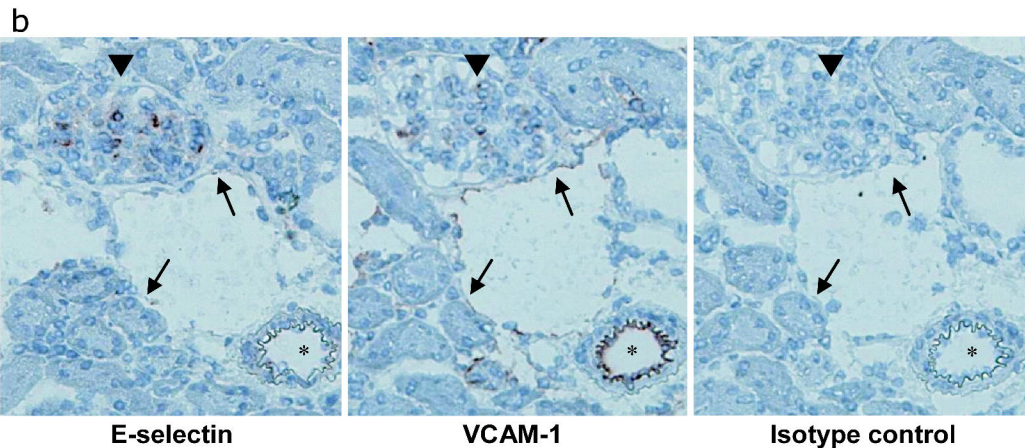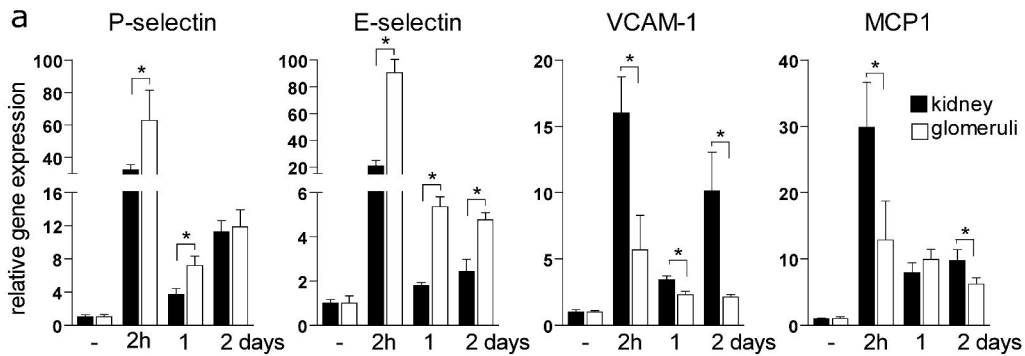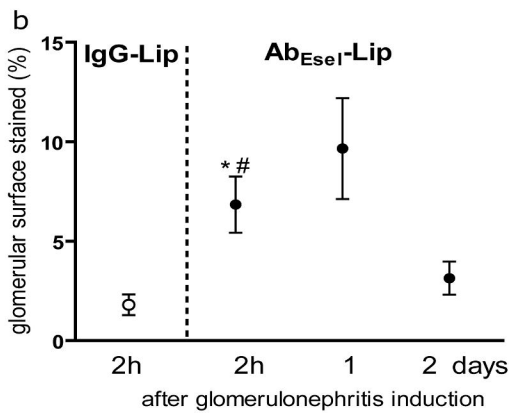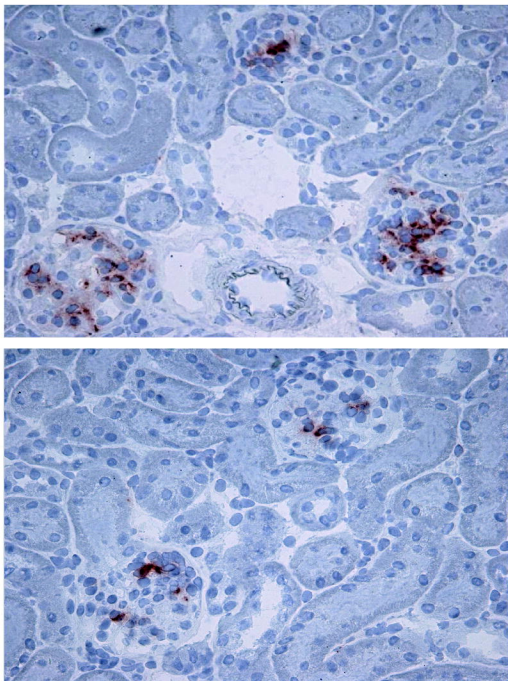
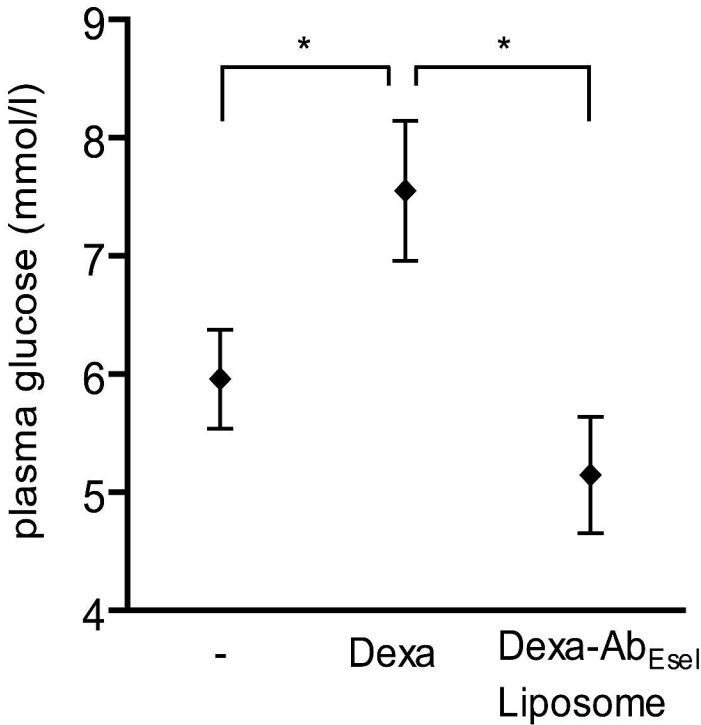**Figure 4**
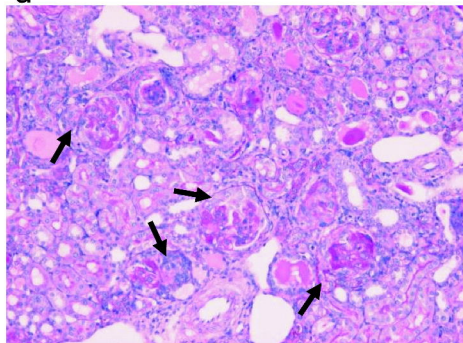
Figure 5

Figure 6

a

b

c

d
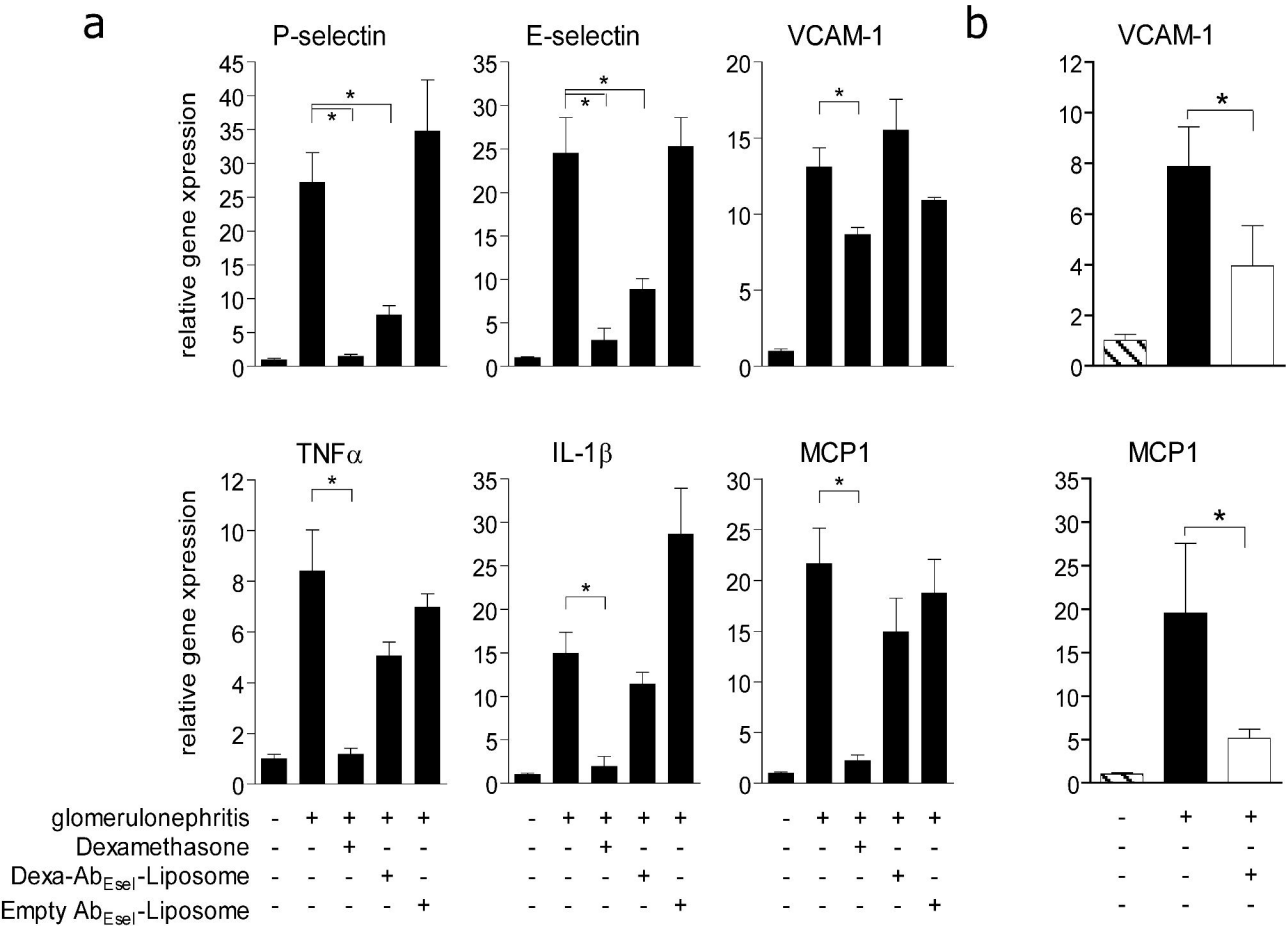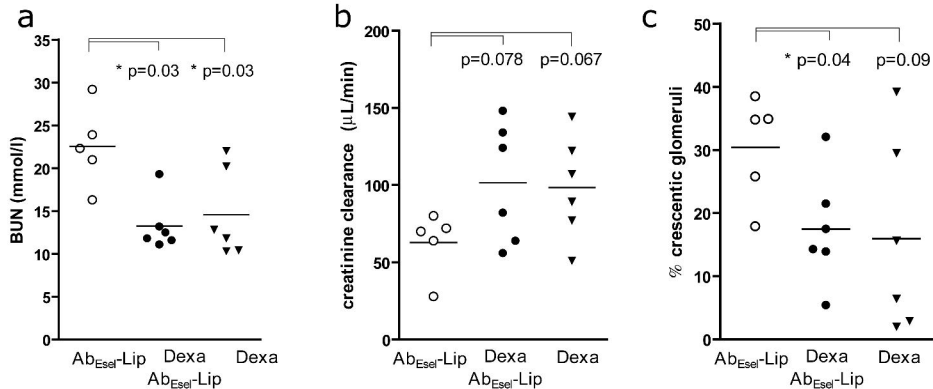
empty Ab$_{Esel}$ liposome
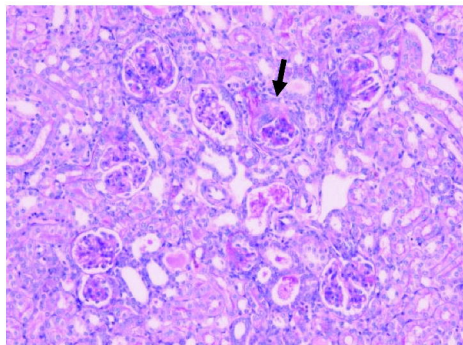
Dexa-Ab$_{Esel}$-liposome

Figure 7

Figure 8